Fluid Flow Distribution in Fractures for a Doublet System in Enhanced Geothermal Systems (EGS)

Pranay Asai, University of Utah; Palash Panja, University of Utah; Raul Velasco, University of Utah; John McLennan, University of Utah; Joseph Moore, University of Utah;

Abstract

Extraction of heat from an enhanced geothermal system (EGS) is a renewable and environmentally benign technology. Process involves circulation of colder water in hot rock through a flow path consisting of injection well, several vertical fractures, and production well. In this process, distribution of water among the vertical fractures is one of the key factors for optimization of heat recovery. Geometry such as dimensions or total flow area and fluid velocity in wells and fractures play major role in the hydrodynamics in the loop. A mathematical model is developed from the analogy of electrical circuit applying Kirchhoff's law to determine the pressure drop between two points. Accordingly, the flow rates through fractures are calculated. Maintenance of sufficient pressure in a fracture is necessary to avoid closure due to horizontal stress. In this model, variation of fracture width with pressure is considered. The impacts of injection rate, well diameter and number of fractures on the distribution of flow in fractures are also investigated in this study. Since the frictional loss along the well decreases with the increase in well diameter, less variations of flow rates in fractures are observed. Similarly, low fluid velocity due to low total flow rate causes less frictional loss, thus more even distributions of flow in the fracture is observed. The number of fractures completed in an EGS is an important parameter for optimization. The flow distribution among the fractures depends on the total number of fractures present in the system. Although, more fractures improve the heat recovery, the cost of completion increases with the number of fracture. The analytical model for flow distribution developed in this study is helpful to evaluate the effectiveness of an EGS and to optimize the completion and operational parameters.

Introduction

For more than a century, geothermal energy has been exploited to produce electricity and provide direct heating. The key to avail this huge resource lies in understanding the geothermal reservoir. Parameters such as the temperature of the reservoir, depth, reservoir size, heat capacity and permeability are a few of the properties that need to be evaluated and studied. This is in addition to the availability of a working fluid. In the absence of mobile water, one way to tap into this huge heat source is by developing an enhanced geothermal system (EGS)[1, 2]. An EGS consists of sets of wells, drilled few hundred meters apart. These wells are interconnected by creating multiple hydraulic fractures. Then, a working fluid (which helps in transporting the heat to the surface) is injected into one or multiple wells, passing through the fractures and brought back to the surface via production wells. While this fluid passes through the fractures, it takes on heat from the formation and brings it out to the surface where it is flashed to steam or run through an organic Rankine cycle heat exchange system. An EGS can consist any number of wells and multiple stages of hydraulically induced fractures.

This study assesses the thermo-hydraulic flow distribution within these hydraulic fractures, in a horizontal doublet system. A doublet system consists of an injection well and a production

well. There would be multiple fractures along the length of the injection well, and these are explicitly connected to the production well. When the working fluid is pumped into the injection well, it is distributed into the fractures and produced via the production well. As the fluid passes through the fractures, it acquires heat from the reservoir. If more fluid is pumped it would extract more heat, although the thermal resource is fundamentally finite in the longer term. To ensure that heat is withdrawn uniformly along the length of the wellbore doublet, it is important to comprehend the flow distribution among the fractures.

There have been many studies to understand the flow patterns in single fracture geothermal system. Zeng et al. [3] evaluated the performance of horizontal doublet system, and concluded that the key factors affecting the energy efficiency are permeability and the water flow rate. Guo et al.[4] studied the thermal drawdown in a single fracture and evaluated the flow patterns in the fracture and its effect on heat production. Al-Rbeawi [5] analyzed the behavior of flow regimes in natural and hydraulically-induced fractured unconventional gas reservoirs and studied the pressure behavior.

Other studies which were carried on multi fractured EGS had a basic assumption that all the fractures take same amount of fluid. Zeng et al. [6] estimated the parameters that affect the power efficiency and life of the EGS by studying the flow in a doublet multi fractured system. Li et al. [7] performed thermal breakdown calculations to optimized the multi-stage EGS by assuming equal flow rates in all the fractures. Wu et al.[8] studied the heat extraction in a vertical doublet system with multiple fractures and also assumed equal flow rates in all the stages. Xia el al. [9] evaluated the design and modeling of a doublet EGS with equal flow rates in all the fractures. As there has been negligible research related to analyzing the flow distribution in a multi fractured enhanced geothermal system, it is important to validate the assumption of equal distribution of fluid.

This study focuses on developing and testing an analytical model to study the flow distribution among the fractures in any given EGS. The mathematical model is derived as an analog to the principle of Kirchhoff's law for current distribution in a closed multi-loop circuit. The resistance to the fluid flow in the pipe and inside the fractures would be used as the criteria to distribute the fluid among the fractures.

Representation of an EGS Doublet System

The EGS system used to carry out this study includes a doublet well system consisting of two horizontal wells, drilled in the same direction, at the same depth and some appropriate distance apart. The wells have multiple fracture stages, along their lengths (see **Figure 1**). Though this is not the most optimized design for a doublet system (a more optimized design for a doublet EGS is given by Shiozawa et al. [10]), it was chosen for its simplicity as a starting point.

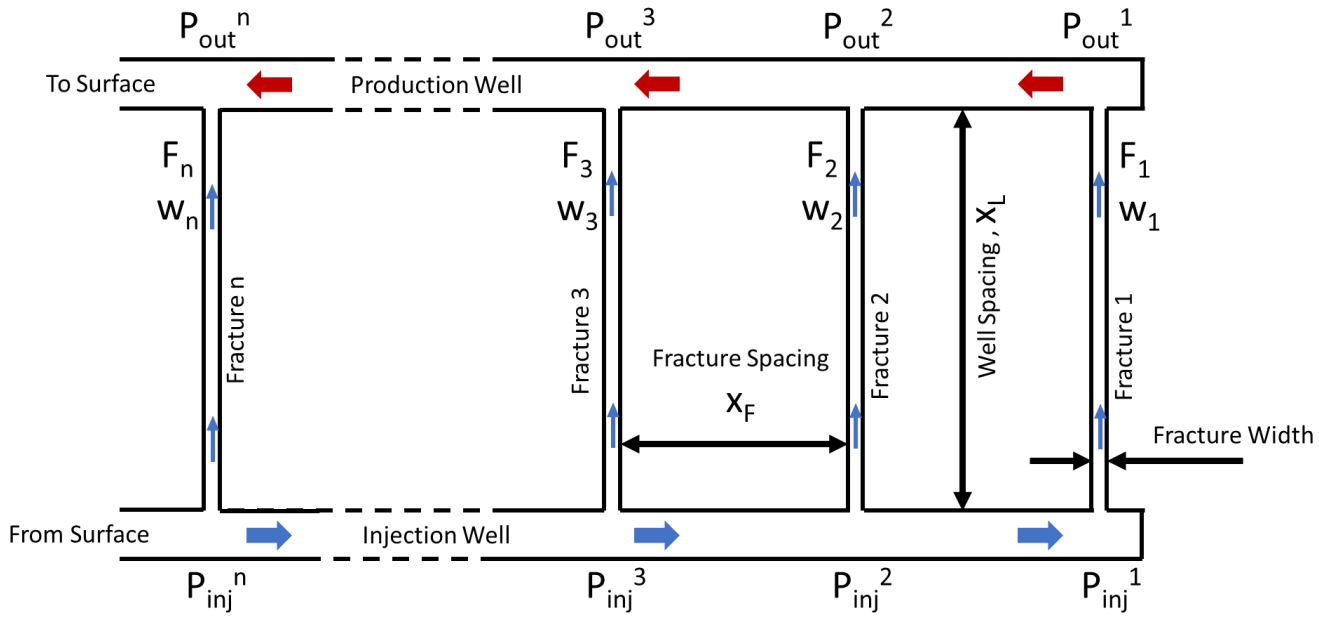

Figure 1: Schematic diagram of a rudimentary EGS – one injector, one producer and n interconnecting infinite conductivity hydraulic fractures

As shown in Figure 1, there are two wells (injection and production wells), and 'n' fractures. The fracture numbering starts from the toe of the wells (end of the wells). 'F_n', represents the fracture number, 'w_n', represents the average width of the n^{th} fracture, 'P_{inj}^{n}', represents the injection pressure at the entrance of the n^{th} fracture, 'P_{out}^{n}', represents the outlet pressure at the n^{th} fracture. 'X_F' represents the fracture spacing and 'X_L', represents the spacing between the two wells.

Each fracture provides a pathway for the fluid to move through the nominally impermeable reservoir and connec presence of natural fractures, turning the system into a complex fracture network. On the other hand, the flow from reservoir pores and through natural fractures is negligible since porosities observed in the geothermal reservoir tend to be very low (around 1%)[11]. In the geothermal context, the heat is transferred to injected water only by conduction from the rock. Hence, to perform the calculations and keep the model simple, a few assumptions were made regarding the fracture shape, fracture spacing, and width of the fracture. Natural fractures are not considered in this study. Hydraulic fractures were considered to be circular [12] (penny shaped in the jargon of hydraulic fracturing and fracture mechanics). This fracture shape is a simplified representation of irregular fracture morphology that can readily be incorporated in the development of analytical fracture flow distribution models. An important advantage of this shape is the quick calculation of fracture area. Other model properties and parameters can be easily computed as well.
The center of this circular facture lies between the two wells and the fracture has a concave shape. Each circular fracture has a diameter equal to the well spacing, and its width varies with the distance from the center. Again, to maintain simplicity in the calculations, an average width was calculated and the fracture was considered to be planar (as shown in **Figure 2**).

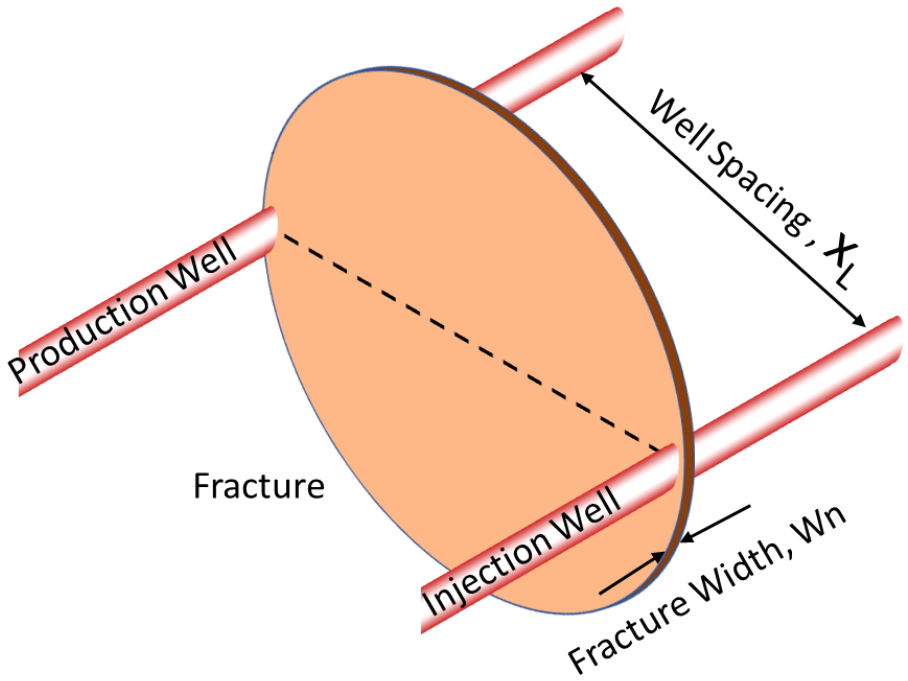

Figure 2: Representation of a planar penny shaped fracture (one of many) for the doublet system

Analogy to Kirchhoff's Voltage law

According to the Kirchhoff's law used for closed electric circuits, division of the current within the loop, takes place according to the resistance present in the circuit. That means, more current would flow where the resistance is the least. The current flowing through a resistance would determine the potential difference across it. Consequently, in a multi loop system having multiple resistances of the same value, each branch would carry an equal amount of current (**Figure 3**) and would have the same amount of potential difference across it.

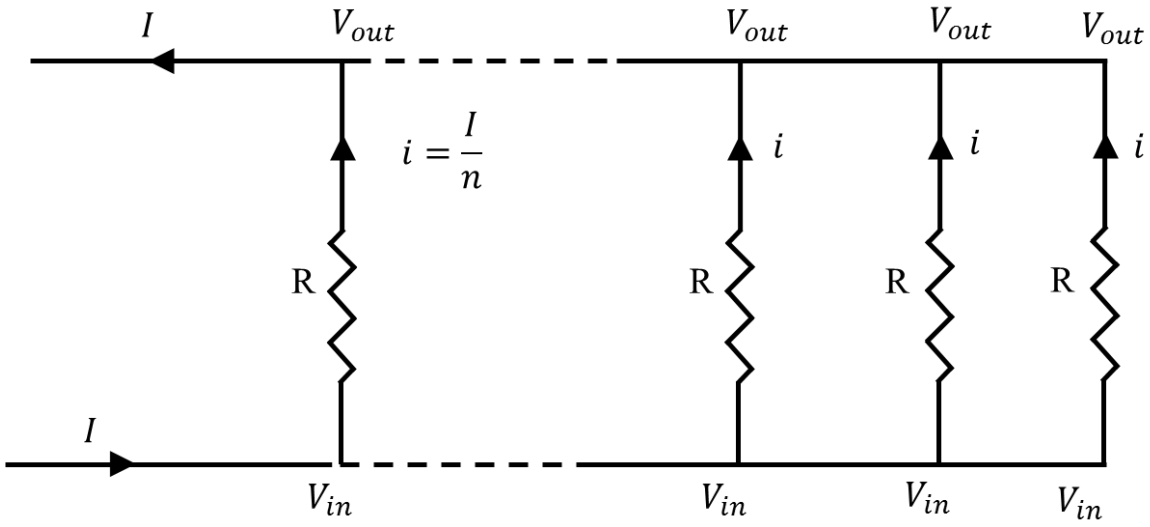

Figure 3: Current distribution in a circuit with 'n' branches of equal resistance

However, when the resistance in the loops are different from each other, the current distribution is governed by Kirchhoff's law. Each branch carries a different amount of current and hence would have a different potential across it (see **Figure 4**).

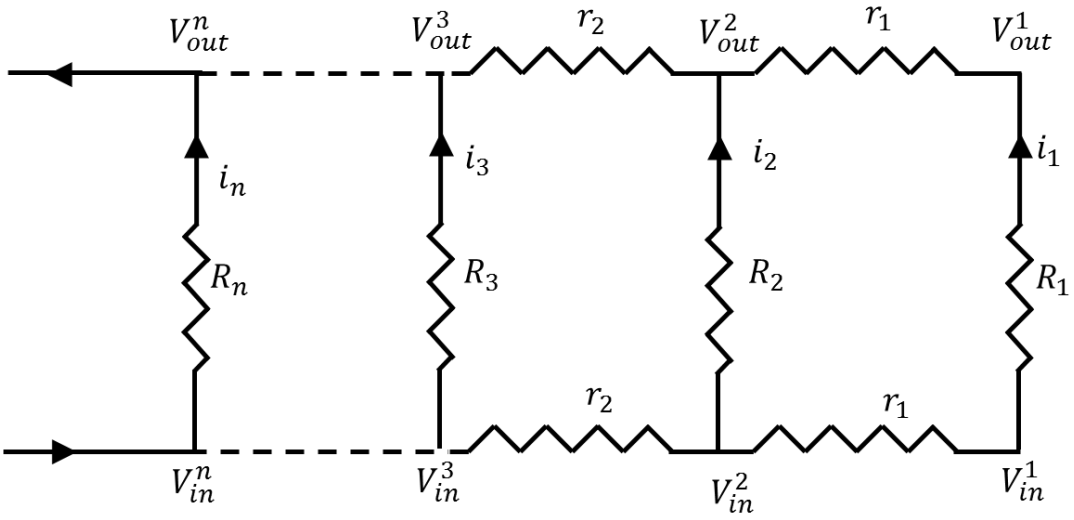

Figure 4: Current distribution in a circuit with multiple resistance

Similarly, when the fluid flows through fractures in a fractured geothermal doublet, it tends to take the path of least resistance. The distribution would depend on the factors causing the resistance to the flow. In a closed loop system with two wells and multiple fractures, the resistance is mainly caused by the frictional force acting opposing the direction of the flow. The fluid flowing in the system is analogous to the current flowing in an electric circuit. The frictional resistance in the fracture and in the injection and production well tubulars is analogous to the resistance in the circuit and the pressure is analogous to the potential difference across the resistance. Neglecting the frictional losses within the wellbore, there would be an equal distribution of fluid in each fracture.

Analogous to the resistance in the electric circuit, the frictional resistance in the well system is dependent on the flow rate. That means the frictional losses would depend on the flow rate in the particular section and thus would change the flow distribution within the fracture. Additional complexities can arise if the flow is turbulent as opposed to laminar (i.e., a non-first order dependence of friction pressure loss on till the volumetric flow rate). Hence, it is necessary to iterate the equations until convergence of the rate and pressure in each fracture is achieved.

Mathematical Representation

To determine the flow distribution among multiple fractures, a simple case consisting of two fractures is considered first. **Figure 5** represents a system consisting of two parallel wells separated horizontally by a distance X_L, with two fractures a distance X_F apart. The fractures are numbered starting from the last fracture at the end of the wells (toe of the well). Fluid would be injected into the injection well at a rate of Q and at an injection pressure of P_{in}. When the system

reaches steady state, the flow rate into the first and second fractures is given as q_1 and q_2, respectively. Fracture one and fracture two will have widths w_1 and w_2, respectively. Since the fractures are circular, it is assumed that the fluid distributes instantaneously over the fracture area and the maximum area of the cross-section in the fracture is taken as the average area of cross-section for the fluid flow across the fracture.[1] The flow across the fracture will cause a drop in the injection pressure due to the friction inside the fracture. In a general situation, for the n^{th} fracture, the frictional pressure drop, $'\Delta P_{frac,\ n}'$, caused by a fluid with a density, $'\rho'$, flowing at a rate, $'q_n'$, inside a fracture whose length is $'X_l'$, with a hydraulic diameter, $'d_h'$, and a cross-sectional area, $'A_f'$, is given by equation 1, where the $'f_{f_{qn}}'$, represents the Fanning friction factor. The coefficient of friction varies with the type of flow inside the fracture and can be estimated accordingly.

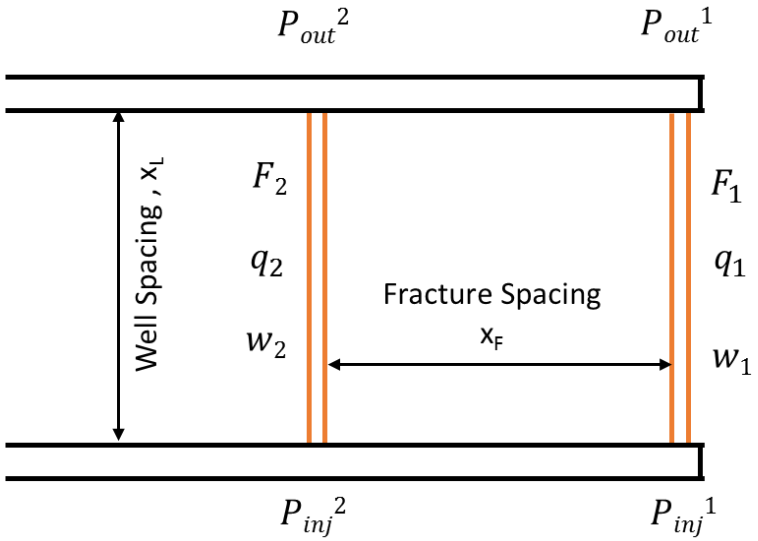

Figure 5: Flow distribution in a two fracture system

$$\Delta P_{frac,\ n} = f_{f_{qn}} \frac{2X_l}{d_h} \rho \left(\frac{q_n}{A_f}\right)^2 \tag{1}$$

Similarly, there is another frictional pressure drop as the fluid passes through the pipe sections between two consecutive fractures. For the section between the n^{th} and $(n-1)^{th}$ fracture, which are $'X_f'$ distance apart, the frictional pressure drop, $'\Delta P_{pipe,\ n}'$, caused by a fluid with a density, $'\rho'$, flowing at a rate, $'q_{p,n}'$, inside a pipe with a hydraulic diameter, $'D_h'$, and a cross-sectional area, $'A_p'$, is given by Equation 2, where $'f_{p_{q_n}}'$, represents the Fanning friction factor for flow in a circular pipe. The coefficient of friction varies depending on the type of flow inside the pipe (laminar, transitional or turbulent) and can be estimated accordingly. Entrance and exit losses and minor losses associated with valves are other components are not considered but could be easily added.

[1] The approximations built into this simplification are acknowledged.

$$\Delta P_{pipe,\ n} = f_{p_{qn}} \frac{2X_f}{D_h} \rho \left(\frac{q_{p,n}}{A_p}\right)^2 \tag{2}$$

Considering the two inlets and two outlets for the fractures as nodal points, Kirchhoff's law for current allocation can be applied to the system. In this case the pressure is analogous to the potential difference, flow rate is analogous to the current and the friction in the pipe and the fractures are analogous to the resistance. The outlet pressure for the second fracture, $'P_{out}^2'$, can be calculated directly by subtracting the pressure drop across the second fracture (see Equation 3) and also by traversing through the pipe section, the first fracture and another pipe section (see Equation 4).

$$P_{out}^2 = P_{in}^2 - f_{F\,q2} \frac{2x_L}{d_h} \rho \left(\frac{q_2}{A_f}\right)^2 \tag{3}$$

$$P_{out}^2 = P_{in}^2 - 2f_{p\,q1} \frac{2x_f}{D_h} \rho \left(\frac{Q - q_2}{A_P}\right)^2 - f_{F\,q1} \frac{2x_L}{d_h} \rho \left(\frac{q_1}{A_f}\right)^2 \tag{4}$$

Since there are many constants in Equation 4, some of these constants can be grouped together as shown in the equation 5 and 6 (these is done for convenience and these are dimensional constants). When Equations 3 and 4 are equated and Equation 5 and Equation 6, are substituted into that relationship the flow rate in the individual fractures is represented by equation 7 and 8.

$$f_{P\,qn} \frac{2\rho x_f}{D_h {A_P}^2} = b_{P\,qn} \tag{5}$$

$$f_{F\,qn} \frac{2\rho x_L}{d_h {A_f}^2} = b_{F\,qn} \tag{6}$$

$$q_2 = Q \frac{\left(\frac{2b_{P\,q1} + b_{F\,q1}}{b_{F\,q2}}\right)^{\frac{1}{2}}}{\left(\frac{2b_{P\,q1} + b_{F\,q1}}{b_{F\,q2}}\right)^{\frac{1}{2}} + 1} \tag{7}$$

$$q_1 = Q \frac{1}{\left(\frac{2b_{P\,q1} + b_{F\,q1}}{b_{F\,q2}}\right)^{\frac{1}{2}} + 1} \tag{8}$$

These equations can be generalized for a system consisting of $'N'$ fractures as shown in **Figure 6**. The flow through the n^{th} fracture can be estimated by Equations 9 and 10. Derivations of these generalized equations are summarized in Appendix A.

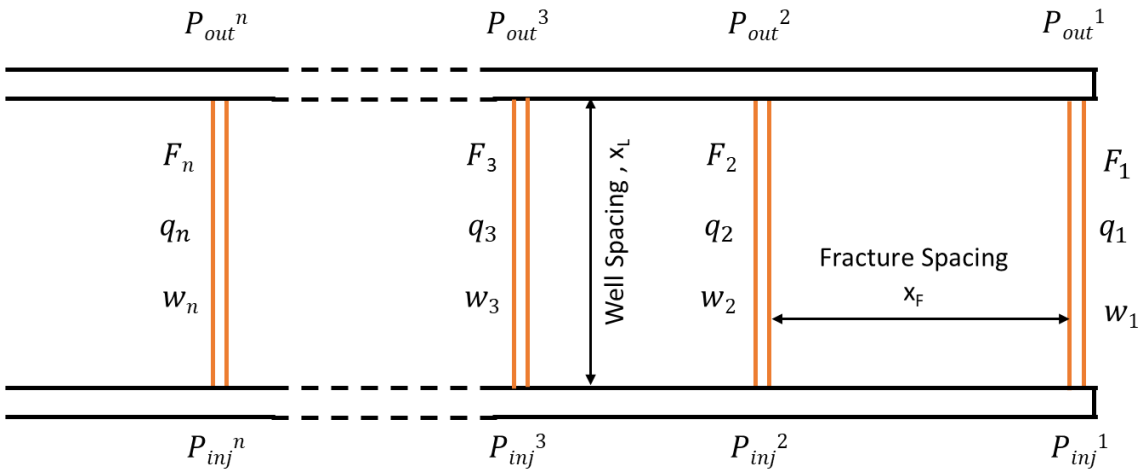

Figure 6: Flow distribution in a multi fracture system consisting n fractures.

$$c_n = \frac{\left(\frac{2b_{P_{q(n-1)}} + b_{F_{q(n-1)}}\left(c_{(n-1)}\right)^2}{b_{F_{qn}}}\right)^{\frac{1}{2}}}{\left(\frac{2b_{P_{q(n-1)}} + b_{F_{q(n-1)}}\left(c_{(n-1)}\right)^2}{b_{F_{qn}}}\right)^{\frac{1}{2}} + 1} \tag{9}$$

$$q_n = \left(Q - \left(\sum_{i=1}^{N} q_{n+1}\right)\right) c_n \tag{10}$$

Where $'n'$ represents the n^{th} fracture and $'N'$ represents the total number of fractures. All the frictional resistances for the n^{th} fracture (resistance in the fracture and the pipe sections), can be grouped together and rewritten as simplified a constant $'c_n'$, to calculate the flow in the $'n^{th}'$ fracture, with the $'c_1 = 1'$.

Since the constants $b_{P_{qn}}$ and $b_{F_{qn}}$ are functions of the friction factors which in turn are functions of the flow rate, it is not possible to write the equations in an explicit form. Multiple iterations need to be carried out by assuming the initial flow distribution in the system and solved until convergence is achieved.

It is important to choose the initial flow distribution carefully because this governs the initial pressure distribution in the system. The inlet pressure at the nearest fracture (the one at the heel of the wells) is the nodal point for the highest pressure and the outlet pressure at the last fracture is the nodal point for lowest pressure in the system to ensure the flow inside the fracture system. Since the width of the fracture depends on the injection and outlet pressures across the fracture and a higher flow rate would cause greater pressure drop, the last fracture (the one at the heel of the wells), will have the highest flow rate. As a result, while choosing the initial distribution, if

higher flow rates are chosen for the fractures at the toe of the well, this might give negative pressure values and will preclude accurate results. Hence, it is important to divide the initial flow in such a way that the first fracture at the toe of the well, gets the minimum amount of fluid so as to reduce the frictional losses in the pipe and within the first fracture at the toe of the well.

One of the way to estimate the initial flow distribution is by dividing the flow using a high degree polynomial distribution. This will ensure that the first fracture (at the toe) takes the least amount of fluid and the last fracture (at the heel) takes the largest amount. The polynomial distribution of the total flow rate,$'Q'$, for the n^{th} fracture in a system consisting of N fractures is shown in Equation 11.

$$q_n = \frac{n^x}{\sum_{i=1}^{N} i^x} Q \tag{11}$$

Equation Validation

Rudimentary equations have been derived for the flow distribution at steady state in a doublet wells system. In order to qualitatively check their validity the relationships were tested with several injection scenarios and the results were analyzed.

The first validation method is to assume that there are no frictional losses in any of the tubulars. This means that the pressure loss term due to pipe friction is zero. This indicates that there is no pressure drop along the length of the pipe and the pressure drop across all the fractures is the same. Applying this criteria to Equation 4, gives Equation 12. When Equation 12 is equated to Equation 3, it gives $'q_1 = q_2'$, meaning all of the fracture will take an equal amount of fluid.

$$P_{out}^2 = P_{in}^2 - f_{F_{q1}} \frac{2x_L}{d_h} \rho \left(\frac{q_1}{A_f}\right)^2 \tag{12}$$

The second method is to assume that the diameter of the pipe is very large. This indicates that the fluid is free to flow inside the pipe with negligible frictional losses. This would again diminish the pressure loss term due to friction in the equation, giving us equal flow in all the fractures.

The third method is to see what happens if the fracture spacing is unrealistically small. As the fracture spacing lies in the numerator of the pipe frictional loss term, it diminishes and gives an almost equal flow rate in all the fractures. This shows that the equations are valid for all type of flow scenarios.

Relation of width with pressure

Flow through a planar fracture is facilitated by the width of the fracture. The permeability of an unpropped fracture is taken to be derived from lubrication theory. Assuming that the fracture is a highly conductive channel (very high permeability – approaching infinite conductivity), the width of the fracture can be defined as the function of injection pressure. For vertical fractures, when the pressure inside the fracture exceeds the minimum total horizontal stress exerted by the

formation, it creates a channel to facilitate the flow. Many studies have been carried out to study the correlation between fracture width and the injection pressure.

One relation between the fracture width and the pressure is given by Witherspoon et al. [13]. It is a cubic law given for a laminar flow between two parallel plates. Equation 13, represents this well-known cubic relationship, with Q as the total flow rate, Δh as the difference in hydraulic head, b as the half width between the two plates and C is a constant that depends on the geometry of the fracture. For a radial flow with well radius of r_w and a fracture radius of r_e, C is given in Equation 14. For a straight line flow in a rectangular fracture of length L and width W, C is given in Equation 15.

$$\frac{Q}{\Delta h} = C(2b)^3 \tag{13}$$

$$C = \left(\frac{2\pi}{ln\left(\frac{r_e}{r_w}\right)}\right)\left(\frac{\rho g}{12\mu}\right) \tag{14}$$

$$C = \left(\frac{W}{L}\right)\left(\frac{\rho g}{12\mu}\right) \tag{15}$$

Combining Equation 13 and 15 for a planar fracture gives Equation 16. This equation gives a relation between the pressure, flow rate and width of the fracture, but it does not implement properties of the formation, such as Young's modulus and Poisson's ratio.

$$\left(\frac{12QL\mu}{\Delta P}\right)^{\frac{1}{4}} = w \tag{16}$$

Another relation was given by the Sneddon and Elliott [14] by studying the opening of Griffith crack under internal pressure. This equation was further modified by Perkins and Kern [12], giving a fracture width equation. This gives a relation between the injection pressure and the width of the fracture and also accounts for the formation properties. According to Sneddon and Elliott, for a three-dimensional, radially symmetrical fracture with radius $'C'$, the width of the fracture at any radius is approximately given by Equation 17. This equation was derived by performing a volumetric balance of injected fluid into the fracture. The fracture is concave in nature and therefore its width varies with radius, with the maximum width being at the center; that is at $r = 0$ (see Equation 18). The average width for the entire fracture can be calculated by taking the volumetric average. The average width of the fracture is shown in Equation 19. In all three equations, the pressure (P_{avg}) used to calculate the average width, is the average of the injection and the outlet pressure for that particular fracture. $'E'$ Represents Young's modulus of the rock, 'ν' represents the Poisson's ratio for the rock and $'\sigma'$ represents the total perpendicular stress acting on the fracture surface due to the formation rock.

$$w_r = \frac{8(P_r - \sigma)C(1 - \nu^2)}{\pi E}\sqrt{1 - \left(\frac{r}{C}\right)^2} \tag{17}$$

$$w_{max} = \frac{8(P_{avg} - \sigma)C(1-\nu^2)}{\pi E} \tag{18}$$

$$w_{avg} = \frac{2}{3} w_{max} = \frac{16(P_{avg} - \sigma)C(1-\nu^2)}{3\pi E} \tag{19}$$

As the fluid passes through the fracture, it loses pressure due to frictional loss. Consequently, the fracture should have the maximum width at the injection point (as the pressure is maximum) and the minimum width at the outlet point (as the pressure is minimum), in a fracture. This forms a trapezoidal shape for the fracture. By taking the area average of the inlet and outlet pressure for a given fracture, Equation 20 gives the average pressure in the fracture, which gives the planar circular fracture with uniform width.

$$P_{avg} = \frac{(2P_{in} + P_{out})}{3} \tag{20}$$

Results and Discussion

We have considered a system wells with a well spacing of $200\ meters$, and consisting of 10 fractures, with a fracture spacing of $50\ meters$. The flowrate in the system was maintained at $500\ m^3/day$, with an injection pressure of $33500\ kPa$. The other properties of the system and properties of the formation are summarized in **Table 1**.

Table 1: Values of properties

Parameter	Value
Flow Rate, Q (m3/day)	500
Diameter of Pipe, Dp (m)	0.1778
Roughness of Pipe, e (mm)	0.0015
Injection Pressure (kPa)	33500
Poisson's Ration, ν	0.33
Young's Modulus, E (kPa)	62052815.6
Injection Pressure, P_{in} (kPa)	33500
Horizontal Stress, σ (kPa)	31670
Number of Fractures	10
Fracture Spacing (m)	50
Well Spacing (m)	200
Radius of the circular fracture (m)	100

The flow inside the fracture is assumed to be laminar and the Fanning friction factor for laminar flow is given by Equation 21, where Re_f is the Reynolds' number

$$f_{F\,qn} = \frac{16}{Re_f} \tag{21}$$

The flow inside the pipe is also assumed to be laminar and the Fanning friction factor for laminar flow inside the cylindrical pipe is approximated by Haaland's equation, Equation 22.

$$\frac{1}{\sqrt{f_{P_{qn}}}} = -1.8 \log\left[\left(\frac{\varepsilon/D}{3.7}\right)^{1.11} + \frac{6.9}{Re_p}\right] \tag{22}$$

Using the foregoing equations and performing 500 iterations gives the result flow distribution for a system with ten fractures (**Table 2**). It is evident that the 10th fracture (at the heel) takes the largest amount of fluid.

Table 2: Flow distribution for 10 fracture system

Frac No.	Flow Rate (m3/day)	Percentage (%)	Width (m)	P in (kPa)
1	20.445	4.089	0.002739	32795.644
2	20.641	4.128	0.002745	32797.822
3	21.318	4.264	0.002764	32805.544
4	22.775	4.555	0.002803	32821.801
5	25.452	5.090	0.002872	32849.942
6	30.132	6.026	0.002980	32894.413
7	38.418	7.684	0.003144	32961.998
8	54.068	10.814	0.003394	33064.454
9	87.679	17.536	0.003785	33225.159
10	179.072	35.814	0.004454	33500.000
Total	500	100		

Effects of number of fractures with fixed flowrate

In this scenario, all of the parameters except the number of fractures, were kept the same as those shown in Table 1. The fluid was injected at a rate of 500 m^3/day and at an injection pressure of 33500 kPa. The number of fractures was varied, from ten to two. As the number of fractures was decreased, the distance between them was increased proportionally, to keep the length of the tubulars equal in the system (see **Figure 7**). The percentage flow distribution among all of the fractures present is plotted in **Figure 8**.

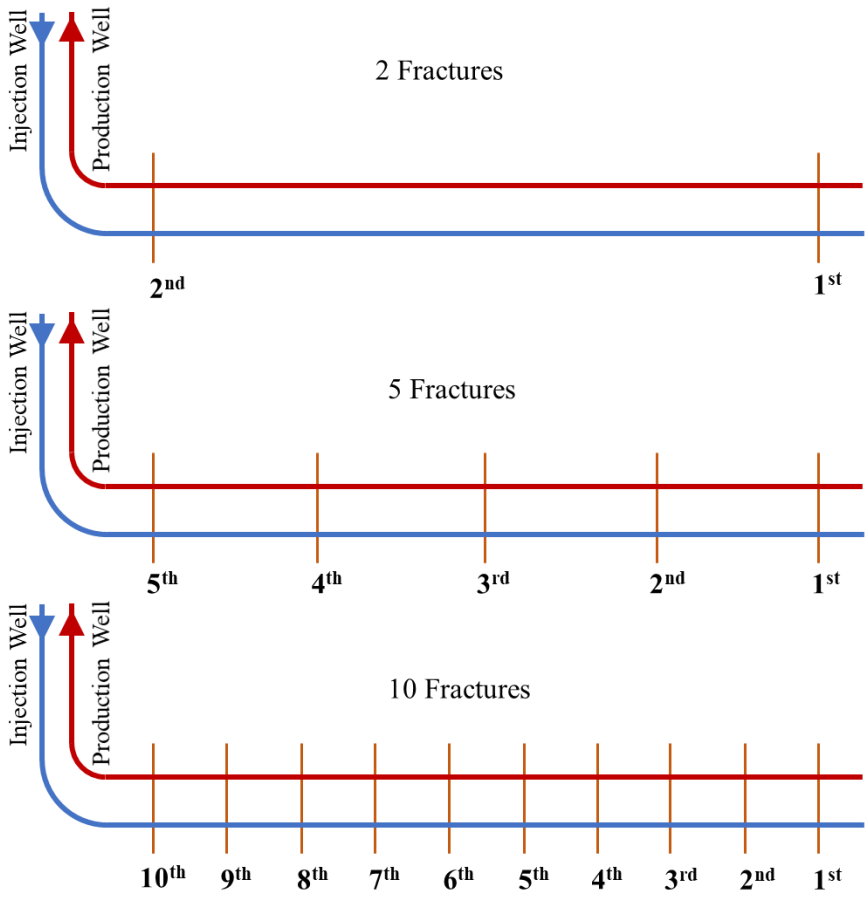

Figure 7: Representation of different number of fractures for the system.

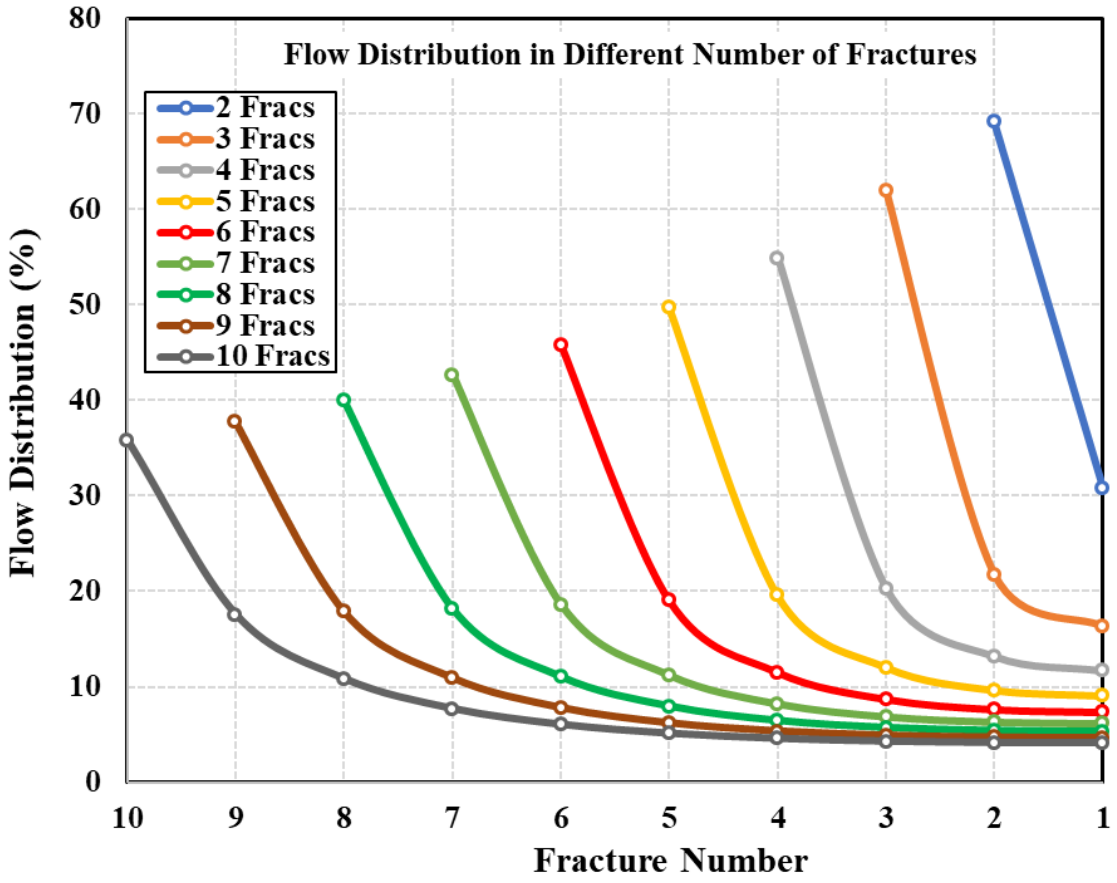

Figure 8: Flow distribution among fractures when the water is injected at different flow rates

In all cases, the first fracture took the least amount of fluid and the last fracture (in the respective system) took the most fluid. As the number of fracture increases in the system the distribution skews towards the last fracture. The system with two fractures had the best distribution with the first fracture taking 70% of fluid and the 2nd fracture (last in this system) taking the remaining fluid. In the system with ten fractures, the first fracture took 4% of the fluid and the 10th fracture took the maximum fluid, amounting to 36% of the total fluid.

As the number of fractures was decreased from ten to two, the overall resistance to flow was reduced. But, since the resistance in the pipe is a function of the flow rate, a preference towards the last fracture is still observed (since it has the least resistance with the maximum width).

Effects of flow rates in fixed number of fractures

An evaluation was conducted to study the effect of variable flow rates ranging from $100\ m^3/day$ to $2000\ m^3/day$, in a system consisting of ten fractures with a constant pressure of $34500\ kPa$. The results are plotted in **Figure 9**.

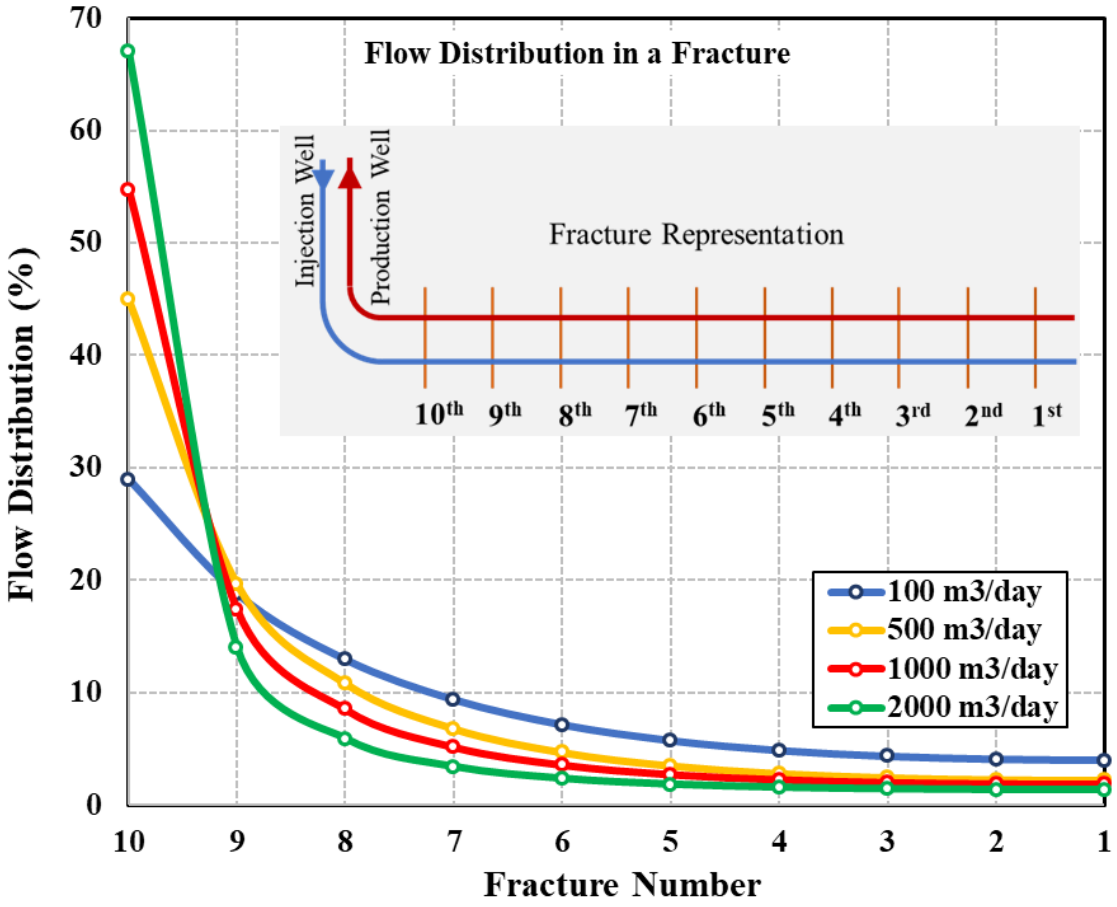

Figure 9: Flow distribution among fractures when water is injected at different flow rates

Again, the last fracture (10^{th} fracture) takes the most fluid of all of the fractures, whereas the 1^{st} fracture (at the toes of the wells) takes the least amount in all the cases. Also, when the flow rate is high ($2000\ m^3/day$), the distribution is much skewed towards the last fracture (at the heel) and reduction in the preferential flow into this last fracture is observed with reduction of the flow rate. It is also observed that the last fracture has the maximum width whereas the first fracture has the minimum width.

This can be explained because when the flow rate is low, the frictional losses in the injection and production tubulars are low as well. This means that there is a low pressure drop between two consecutive fractures and hence gives a fairly even distribution amongst the fractures. Alternatively, when the flow rate is high, the frictional losses are high and this creates high resistance to flow in the tubulars, and only a small amount of water circulates into the other fractures. Hence all of the fluid tries to enter into the first fracture it encounters while being injected (that is the last fracture in the system with numbering beginning from the toe of the well). Another reason the fluid tries to enter into the fracture nearest to the heel is because it has maximum width and as the width is a function of pressure inside the fracture, the first fracture at the heel, where the injection pressure is maximum leading to the maximum width.

Effects of well diameter with fixed number of fractures and flow rate

To study the effect of pipe diameter on the flow distribution in a doublet system, all of the parameters were kept the same as in Table 1, except that the diameter of the injection and production well were varied. The diameter of each tubular section was varied from 6 inches to 10 inches, and the flow distribution amongst the 10 fractures was plotted in **Figure 10**.

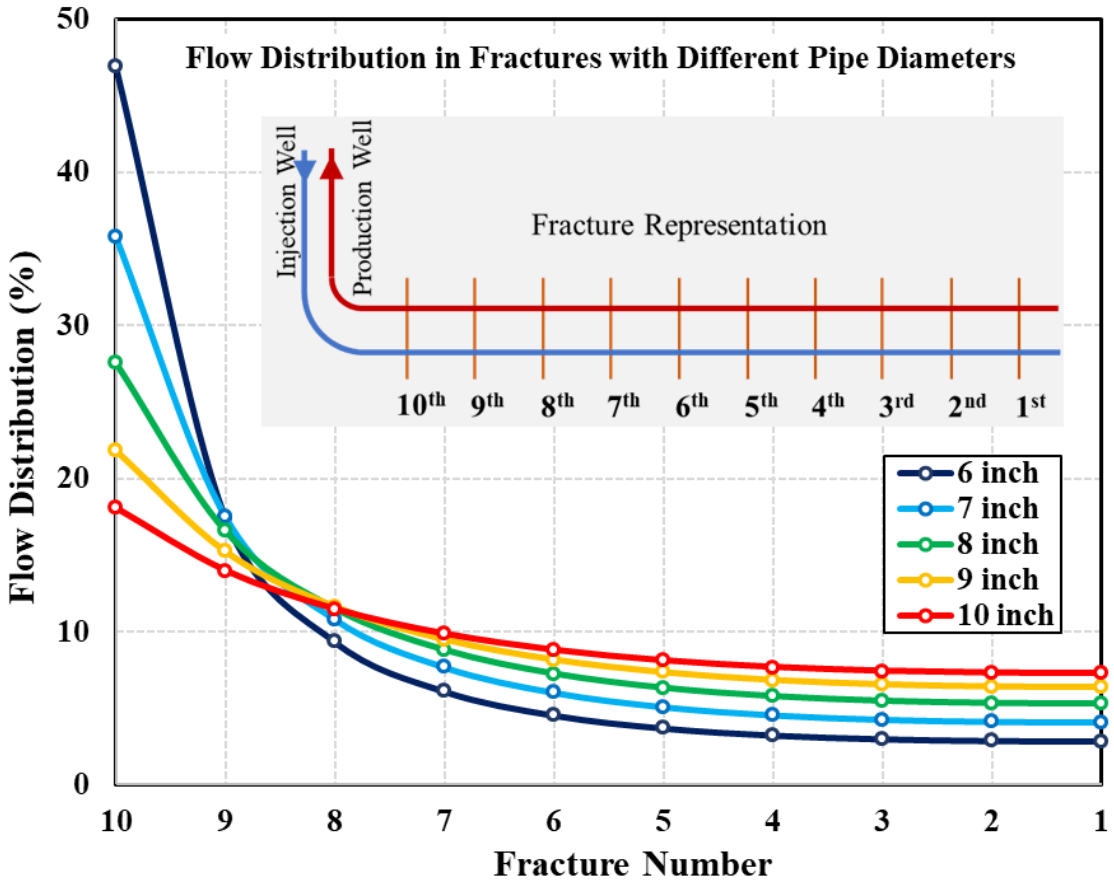

Figure 10: Flow distribution among fractures when the well bore diameter is changed

It was observed that the pipe with least diameter has a distribution that is largely skewed towards the last fracture (10^{th} fracture) and the pipe with the maximum diameter had fairly even distribution among the fractures.

The difference in the flow distribution with diameter of the pipe is observed because of the resistance in the pipes. A small diameter would restrict the fluid flow and create significant frictional resistance between consecutive fractures, reducing the tendency to acquire more fluid. But when the diameter of the pipe is fairly large, the resistance inside the pipe is minimized and the distribution of fluid is even among all of the fractures.

Conclusions

It is important to plan for and design fracture spacing to control the flow distribution in an EGS, to insure that the fluid is evenly distributed in all of the fractures so that the heat is being extracted from the complete reservoir.

Equations 9 and 10 are the basic relationships. These are flexible enough to be applied to any doublet system (drilled in the same direction) and study the flow distribution in it. Since the resistance to flow is a function of the volumetric flow rate, the system of equations needs to be iterated until a converged solution is obtained. The other parameters required to solve these equations include a relation between the injection pressure and width of the fracture, a relationship to calculate the frictional loss in the tubulars, a relationship for calculating the frictional loss in the fracture and a reasonable initial fluid distribution in the fractures (can be calculated by considering a polynomial distribution).

There are many factors that affect the fluid distribution among the fracture. The most important are the injection pressure and the injection flow rate. Optimization of the flow (even distribution) is possible and can be achieved by manipulating the controllable engineering parameters.

This flow distribution method based on Kirchhoff's law, can be applied to any kind of multi-well system to find the flow distribution in multiple fractures. A further study can be carried out investigating the effect of different fracture sizes and shapes (by representing them as different resistance) on the flow distribution in a given system.

List of symbols

Symbols	Description
F_n	Fracture number, starting from toe of the well
w_n	Width of the n^{th} fracture, m
X_L	Well spacing, m
X_F	Fracture spacing, m
Q	Total flow rate in the system, m^3/day
q_n	Flow rate in the n^{th} fracture, m^3/day
R_n	Resistance number, starting from last branch of the circuit, Ohm
V_{in}^n	Voltage at inlet of the n^{th} resistance, Volts
V_{out}^n	Voltage at outlet of the n^{th} resistance, Volts
i_n	Current in the n^{th} resistance, Amperes
ρ	Density of fluid, kg/m^3
A_p	Cross sectional area of well, m^2
A_f	Maximum cross sectional area of fracture, m^2
g	Magnitude of gravitational force, m/s^2
μ	Fluid viscosity, Pa.s
σ	Total perpendicular stress acting on the fracture, Pa
E	Young's modulus, Pa
ν	Poisson's ratio
ε	Roughness of the pipe, m

References

[1] A. S. Batchelor, "The Creation of Hot Dry Rock Systems by Combined Explosive and Hydraulic Fracturing," presented at the Proceedings of the International Conference on Geothermal Energy, May, Florence, Italy 1981.

[2] F. H. Cornet, "Experimental investigations of forced fluid flow through a granite rock mass," presented at the Proceedings of 4th International Seminar on the Results of EC Geothermal Energy Demonstration, April 27-30, Florence, Italy, 1989.

[3] Y.-C. Zeng, N.-Y. Wu, Z. Su, X.-X. Wang, and J. Hu, "Numerical simulation of heat production potential from hot dry rock by water circulating through a novel single vertical fracture at Desert Peak geothermal field," *Energy,* vol. 63, pp. 268-282, 2013.

[4] B. Guo, P. Fu, Y. Hao, C. A. Peters, and C. R. Carrigan, "Thermal drawdown-induced flow channeling in a single fracture in EGS," *Geothermics,* vol. 61, pp. 46-62, 2016.

[5] S. Al-Rbeawi, "Analysis of pressure behaviors and flow regimes of naturally and hydraulically fractured unconventional gas reservoirs using multi-linear flow regimes approach," *Journal of Natural Gas Science and Engineering,* vol. 45, pp. 637-658, 2017.

[6] Y. Zeng, L. Tang, N. Wu, and Y. Cao, "Analysis of influencing factors of production performance of enhanced geothermal system: A case study at Yangbajing geothermal field," *Energy,* vol. 127, pp. 218-235, 2017.

[7] T. Li, S. Shiozawa, and M. W. McClure, "Thermal breakthrough calculations to optimize design of a multiple-stage Enhanced Geothermal System," *Geothermics,* vol. 64, pp. 455-465, 2016.

[8] B. Wu, X. Zhang, R. G. Jeffrey, A. P. Bunger, and S. Jia, "A simplified model for heat extraction by circulating fluid through a closed-loop multiple-fracture enhanced geothermal system," *Applied Energy,* vol. 183, pp. 1664-1681, 2016.

[9] Y. Xia, M. Plummer, E. Mattson, R. Podgorney, and A. Ghassemi, "Design, modeling, and evaluation of a doublet heat extraction model in enhanced geothermal systems," *Renewable Energy,* vol. 105, pp. 232-247, 2017.

[10] S. Shiozawa and M. McClure, "EGS designs with horizontal wells, multiple stages, and proppant," presented at the Thirty-Ninth Workshop on Geothermal Reservoir Engineering, Stanford University, Stanford, California, February 24-26, 2014.

[11] P. Asai, P. Panja, J. McLennan, and J. Moore, "Performance evaluation of enhanced geothermal system (EGS): Surrogate models, sensitivity study and ranking key parameters," *Renewable Energy,* vol. 122, pp. 184-195, 2018.

[12] T. K. Perkins and L. R. Kern, "Widths of Hydraulic Fractures," *Journal of Petroleum Technology,* vol. 13, pp. 937-949, 1961/9/1/ 1961.

[13] P. A. Witherspoon, J. S. Y. Wang, K. Iwai, and J. E. Gale, "Validity of Cubic Law for Fluid Flow in a Deformable Rock Fracture," *Water Resources Research,* vol. 16, pp. 1016-1024, 1980.

[14] I. N. Sneddon and H. A. Elliott, "The Opening of a Griffith Crack under Internal Pressure," *Quarterly of Applied Mathematics,* vol. 4, pp. 262-267, 1946.

Appendix A

For flow distribution in a three fracture system as shown in **Figure A1**, can be derived by using the pressure drop equations given by Equation A1 (pressure drop across a fracture) and Equation A2 (pressure drop across a pipe section between two fractures).

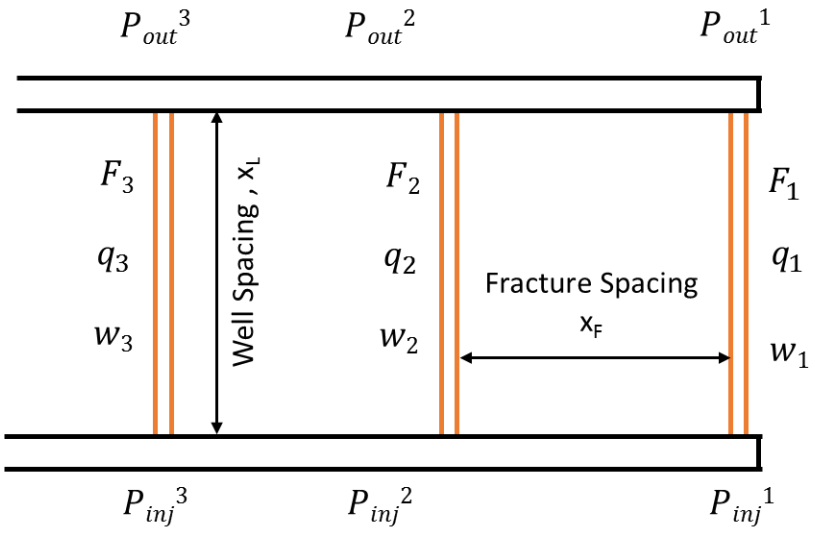

Figure A1: Flow distribution in a three fracture system.

$$\Delta P_{frac,\ n} = f_{f_{qn}} \frac{2X_l}{d_h} \rho \left(\frac{q_n}{A_f}\right)^2 = b_{F_{qn}} (q_n)^2 \qquad (A.1)$$

$$\Delta P_{pipe,\ n} = f_{p_{q_n}} \frac{2X_f}{D_h} \rho \left(\frac{q_{p,n}}{A_p}\right)^2 = b_{P_{qn}} (q_{p,n})^2 \qquad (A.2)$$

So the considering only last two fractures (1 and 2), the flow distribution can be given according to equation 7 and 8. Equation A3 and A4 represents the flow distribution in the last two fractures in a 3 fracture system.

For 3 Fracture system

$$q_1 = (Q - q_3) \frac{1}{\left(\frac{2b_{P_{q1}} + b_{F_{q1}}}{b_{F_{q2}}}\right)^{\frac{1}{2}} + 1} \qquad (A.3)$$

$$q_2 = (Q - q_3)\frac{\left(\frac{2b_{P_{q1}} + b_{F_{q1}}}{b_{F_{q2}}}\right)^{\frac{1}{2}}}{\left(\frac{2b_{P_{q1}} + b_{F_{q1}}}{b_{F_{q2}}}\right)^{\frac{1}{2}} + 1} \quad (A.4)$$

The resistance in the equation A4, can be clubbed together to get an equivalent resistance $'c_2'$, as shown in Equation A5.

$$c_2 = \frac{\left(\frac{2b_{P_{q1}} + b_{F_{q1}}}{b_{F_{q2}}}\right)^{\frac{1}{2}}}{\left(\frac{2b_{P_{q1}} + b_{F_{q1}}}{b_{F_{q2}}}\right)^{\frac{1}{2}} + 1} \quad (A.5)$$

So the flow in second fracture is given as Equation A6.

$$q_2 = (Q - q_3)c_2 \quad (A.6)$$

Now for the third fracture ${P_{out}}^3$, can be calculated directly by subtracting the pressure drop across the third fracture (see Equation A7) and also by traversing through the pipe section, the second fracture and another pipe section (see Equation A8).

$${P_{out}}^3 = {P_{in}}^3 - b_{F_{q3}}(q_3)^2 \quad (A.7)$$

$${P_{out}}^3 = {P_{in}}^3 - 2b_{P_{qn}}(Q - q_3)^2 - b_{F_{q3}}{q_2}^2 \quad (A.8)$$

Equating equation A7 and A8 gives Equation A9

$$2b_{P_{q2}}(Q - q_3)^2 + b_{F_{q2}}{q_2}^2 = b_{F_{q3}}{q_3}^2 \quad (A.9)$$

Substituting equation A6 in equation A9 gives Equation A10

$$2b_{P_{q2}}(Q - q_3)^2 + b_{F_{q2}}(Q - q_3)^2(c_2)^2 = b_{F_{q3}}{q_3}^2 \quad (A.10)$$

Equation A10 can be solved further to calculate value of q_3. The value of q_3 is given by Equation 11.

$$q_3 = Q\frac{\left(\frac{2b_{P_{q2}} + b_{F_{q2}}(c_2)^2}{b_{F_{q3}}}\right)^{\frac{1}{2}}}{\left(\frac{2b_{P_{q2}} + b_{F_{q2}}(c_2)^2}{b_{F_{q3}}}\right)^{\frac{1}{2}} + 1} \quad (A.11)$$

Equation A11 for q_3, is in the same form as equation A4 for q_2. Hence a generalized equation can be written in the form of equivalent resistance for the n^{th} fracture as shown in Equation A12 and the flow through the n^{th} fracture is given by Equation A13.

$$c_n = \frac{\left(\frac{2b_{P_{q(n-1)}} + b_{F_{q(n-1)}}\left(c_{(n-1)}\right)^2}{b_{F_{qn}}}\right)^{\frac{1}{2}}}{\left(\frac{2b_{P_{q(n-1)}} + b_{F_{q(n-1)}}\left(c_{(n-1)}\right)^2}{b_{F_{qn}}}\right)^{\frac{1}{2}} + 1} \qquad (A.12)$$

$$q_n = \left(Q - \left(\sum_{i=n}^{N} q_{n+1}\right)\right) c_n \qquad (A.13)$$

For the first fracture, there is no pipe section so, $b_{P_{q1}} = 0$. This implies that the value of c_1 is '1' to get equation A3 from the general form.